Ab Initio Study of the S_N2 Reaction $CH_3Cl + Cl^- \rightarrow Cl^- + CH_3Cl$ in Supercritical Water with the Polarizable Continuum Model

Christian Silvio Pomelli

Scuola Normale Superiore, Piazza dei Cavalieri, 7 56126 Pisa, Italy

Jacopo Tomasi*

Dipartimento di Chimica e di Chimica Industriale, Universitá degli studi di Pisa, Via Risorgimento, 35 56124 Pisa, Italy

Received: August 5, 1996; In Final Form: November 28, 1996[⊗]

We present some calculations for an S_N2 reaction in ambient and supercritical water performed with a continuum method for solvation, the polarizable continuum model (PCM). PCM allows us to perform quantum mechanical (QM) *ab initio* calculations at almost all the levels of the QM theory and allows us to treat solvent-separated solutes on the same footing as a tight reacting system. Both features are here exploited. The results indicate that the standard PCM version is able to reproduce computer simulation results at a good level of accuracy, with the exception of a specific range of $P-T$ values of supercritical water characterized by a large isothermal compressibility. For calculations in this $P-T$ range we present a PCM formulation giving results in good agreement with results from simulations.

1. Introduction

In recent years supercritical water (SCW) has attracted attention as a medium for chemical reactions because of the interesting, and unique, properties it exhibits.[1,2] To study chemical reactions in SCW with theoretical and computational tools, one has to fully understand the properties of SCW at the microscopic level, both in the bulk and near the solute. This information mainly comes from simulation studies because experimental data give indirect information on this topic and are hard to obtain at the pressure−temperature range at which SCW exists.

There are several computer simulation studies on SCW giving information about the structure of SCW around polar and nonpolar solutes.[3−12] The resulting picture of the local structure of SCW around solutes gives enough elements to draw continuum solvent models of SCW to be used to study solvation effects on single solutes or on chemical reactions.

We recall that modern continuum models have great potential in describing molecular systems in solution[13] because they may also use a good level of the quantum mechanical description of the system. To be properly applied, they require, however, a previous knowledge of the effect of the solute on the local distribution of the solvent, a knowledge that must derived from other sources, such as experimental or simulation studies. This has been done for water at ambient condition (AW) as well as for many other solvents, and modern continuum methods are nowadays gaining wide popularity in the study of complex chemical events, such as reactions in liquids at ambient pressure and temperature (for a recent review, see Tomasi et al.[14]).

The elaboration of continuum models for supercritical liquids is at its initial stage. The only model explicitly addressed to treat SCW we know is due to Luo and Tucker.[15] This model takes into specific account the phenomena of local clustering of SCW around charged solutes put in evidence by simulations. We shall examine the details of this model later.

Computational studies on chemical reactions in SCW are scarce. We know a set of papers regarding molecular dynamics simulation on an S_N2 reaction,[8,11,12] complemented by a continuum model study,[16] and some studies on the anisole hydrolysis, using a continuum model.[15,17] We have already mentioned the new continuum model proposed in ref 15. The other studies[16,17] used the DelPhi program[18] that is based on a uniform dielectric continuum model. Both DelPhi and the new model for SCW use a classical description of the solute expressed in terms of point charges.

In this paper we reconsider the same S_N2 reaction studied by Johnston, Rossky, and co-workers[8,11,12] using the *ab initio* polarizable continuum model (PCM) procedures. PCM has greatly evolved from its initial formulation[19] and now presents several additional features making it particularly suitable for studying chemical reactions, even in media exhibiting considerable local disturbances in the distribution of the solute (the so-called cybotactic effects).

We shall report here a selection of PCM features that are interesting in the study of chemical reactions. (1) It is applicable to all levels of quantum mechanical (QM) theory from semiempirical SCF methods to *ab initio* methods including correlation (MBPT, CASSCF-CI, etc.). (2) It is able to describe, at the same level of accuracy, both connected and disconnected molecular systems (we indicate as disconnected the systems in which two or more partners of a reaction are separated by the solvent). (3) It may be used with both isotropic and anisotropic solvent (the anisotropies of interest here are of a local nature related to the cybotactic effect, such as solvent clustering, electrostriction, dielectric saturation, etc.[20]). (4) The basic energetic quantity is the free energy $G(R)$, which, in the usual Born−Oppenheimer approximation, defines a free energy hypersurface in the space spanned by the nuclear coordinates $\{R\}$ on which the reaction proceeds. $G(R)$ is partitioned into components that can be evaluated with separate calculations:

$$G(R) = G_{el}(R) + G_{rep}(R) + G_{dis}(R) + G_{cav}(R) \qquad (1)$$

An additional term depends on the local shape of the $G(R)$

* To whom correspondence should be addressed. E-mail: tomasi@dcci.unipi.it.

⊗ Abstract published in *Advance ACS Abstracts,* April 15, 1997.

S1089-5639(96)02358-4 CCC: $14.00 © 1997 American Chemical Society

hypersurface and collects entropic contributions due to internal motions of the solute M:

$$G_{tot}(R) = G(R) + G_{Mm}(R) \quad (2)$$

The contributions reported in eq 1 are related, in the order, to electrostatic interaction within the solute and between the solute and the continuum solvent, Pauli repulsion solute−solvents effects, dispersion solute effects, and reversible work spent to form a cavity in the solvent (or cavities) with the appropriate shape to accommodate the solute (or solutes). Details of this partition, and of the computational methods used in PCM, can be found in several papers; see, for example, ref 13. Here, we shall make some comments on G_{el} alone.

G_{el} is defined as the reversible work spent to collect noninteracting electrons and nuclei of the solute M within the cavity, taking into account all mutual polarization effects, including mutual solute−solvent polarization. It is obtained by solving an appropriate Schrödinger equation containing a solute−solvent interaction potential that depends both on the solute charge distribution and on the characteristics of the medium. G_{el} can be thus compared to the total energy of M in vacuo, E_{tot}. The difference of these two quantities gives the electrostatic component of the solvation energy:

$$\Delta G_{el}(R) = G_{el}(R) - E_{tot}(R) \quad (3)$$

The total solvation energy can be obtained by adding to ΔG_{el} the other terms of eq 1, and the difference of the internal motions of *M*, computed in vacuum and in solution:

$$\Delta G_{sol}(R) = \Delta G_{el}(R) + G_{rep}(R) + G_{dis}(R) + G_{cav}(R) + \Delta G_{Mm}(R) \quad (4)$$

G_{el} is sensitive to the characteristics of the continuum solvent distribution. The local anisotropies introduced at point 3 may have a remarkable effect on G_{el}. The effects they have on G_{rep} and G_{dis} are of a minor extent.

PCM methods have been used on several occasions to study S_N2 reactions in liquids at ambient pressure and temperature.[21−26] Some of these studies go beyond the static description of the reaction profile and include dynamical and solvent fluctuation effects.[23,24] In the present paper we shall limit ourselves to the study of static energy profile. By use of standard PCM procedure, the description of the $Cl^- + CH_3Cl$ reaction in water faithfully corresponds to the Monte Carlo energy profile given by Jorgensen and co-workers[27] in a well-known paper that initiated studies on reaction in solution using combined QM and computer simulation techniques.

The long experience in the use of PCM on systems at ambient conditions, and the comparison with computer simulations and with experimental results, leads us to confirm the opinion that the selection of cavity radii used in standard PCM quite well compensates the local cybotactic effects[28] for neutral and anionic solutes. There is no comparable experience for neutral and anionic solutes in supercritical liquids. These fluids, and SCW in particular, exhibit in some region of their phase diagram a large isothermal compressibility and hence larger cybotactic effects.

The main objectives of this paper can be stated as follows: first, to check if the standard version of PCM, with only the inclusion of the appropriate experimental values of the dielectric constant ϵ and of the density *d*, is sufficient to reproduce the reaction energy profile given by molecular dynamics; second, to introduce, and to check, a modified PCM procedure where cybotactic effects expressed as solvent clustering are explicitly introduced.

TABLE 1: Thermodynamic and Electrostatic Properties of Water in Various Conditions

solvent	*T*, K	T_r	*d*, kg/L	d_r	ϵ
AW	298	0.5	1.00	3.1	78.39
SCW1	647	1.0	0.48	1.5	9.73
SCW2	647	1.0	0.16	0.5	2.66
SCW3	841	1.3	0.16	0.5	2.24

2. Standard Model

We shall start our study with a simple formulation of PCM for the reasons we have just expressed.

The reacting system M is described by taking as the solute the nominal system $Cl^- + CH_3Cl$ described at the *ab initio* SCF level along all the reaction coordinates r_c (to be defined below) with geometry optimization. The solute is inserted into a cavity (or a couple of cavities at larger $|r_c|$ values) composed of spheres centered on nuclei of M with radii equal to

$$fR_{vdw} \quad (5)$$

The cavity is smoothed and refined, where necessary, by adding additional spheres to describe better the space where solvent is excluded. These cavities are built by using the GEPOL procedure, documented in other papers.[29,30] The addition of spheres is automatically done in this procedure.

Continuum solvation methods require a correction to account for the portion of the electronic charge distribution of M lying outside the cavity volume. This correction is performed in PCM by renormalizing, at the appropriate value (obtained from electrostatic theorems), the apparent surface charge (ASC) used as the source of the solvent reaction potential.

This renormalization can be done in several ways[31] depending on the electric properties of the solute as well as on the PCM procedure we are using. Being here the first time that the most recent PCM version[31] has been used for reacting systems where the solvent-separated components bear a different total charge (−1 for Cl^- and 0 for CH_3Cl), we have introduced a novel renormalization procedure, different from that used in previous papers and those of refs 23, 24, 25, and 28 on S_N2 reactions. This procedure is described in the appendix to this paper.

The solvent is here described as an isotropic medium characterized by bulk parameters, dielectric constant ϵ, and density *d* at each given $P-T$ value. These values, which can be found in Archer and Wang's collection of data,[32] are reported in Table 1 for the three supercritical cases here considered.

The free energy $G(R)$ is computed according to eq 1 with each term separately computed. The electrostatic contribution G_{el} is computed according to the method of Cammi and Tomasi.[31] As we have said, it also includes the work of formation of M in the suitable cavity, starting from noninteracting electrons and nuclei. G_{dis} and G_{rep} are computed according to ref 33, G_{cav} using the Pierotti−Claverie formula,[34] and G_{Mm}, which includes molecular motions of M, with standard statistical mechanics techniques at the appropriate temperature. A geometry optimization of M has been performed on the whole $G(R)$ of eq 1 with G_{el} computed at the SCF level. Geometry optimization also has been performed at MP2 level only for reagents and the transition state. The last set of geometries has been used to compute $G(R)$ at the following levels of the quantum theory: MP2, MP4, QCISD.

3. Modified Procedure

To introduce cybotactic effects we shall abandon for the calculation of G_{el} the procedure based on apparent surface

charges (ASC) in favor of another procedure based on apparent volume charges (AVC). The ASC problem can be solved with the aid of the boundary element method (BEM), while the AVC problems require the use of a finite element method (FEM).[35] FEM procedures are more difficult to handle than BEM procedures; when ϵ is a constant over the whole body of the continuum medium, an FEM procedure merges into a BEM problem. We shall adopt here, with suitable modifications, an FEM−PCM procedure elaborated and tested for other problems.[36,37]

The bulk of the dielectric is divided into regions of volume V_j, with reference to the center of charge P_0 of solute atoms. To divide the volume, we resort to the partition of the cavity surface in the same tesserae we have used in the standard PCM model. For each tessera T_l we adopt the following procedure. (1) A new sphere S_0 having its center in P_0 is defined to have the representative point of T_l on its surface. (2) The tessera T_l is projected onto the sphere S_0, thus obtaining a new tessera T_l' with area A_l'. (3) A set of concentric spheres $\{S_k\}$ (where $k = 1, 2, ..., k_{max}$) having the same center is defined, starting from S_0 and with radii exhibiting linear increments

$$r_k = r_0 + \frac{k}{k_{max}}(r_{k_{max}} - r_0) \tag{6}$$

The program has both k_{max} and $r_{k_{max}}$ as input data. (4) The tessera T_l' is projected onto the set of spheres $\{S_k\}$, giving origin to regions of volume

$$V_{lk} = \frac{4\pi}{3}(r_k^3 - r_{k-1}^3)\frac{A_l'}{4\pi r_0^2} \tag{7}$$

The representative point is chosen at the middle of each portion of volume.

The AVCs are given in terms of the local value of the polarization charge density

$$\rho_{pol}(\vec{p}) = \frac{\epsilon(\vec{p}) - 1}{\epsilon(\vec{p})}\rho_{sol}(\vec{p}) - \frac{1}{4\pi\epsilon(\vec{p})}[\nabla\epsilon(\vec{p})]\cdot\vec{E}(\vec{p}) \tag{8}$$

where $\vec{p}$ is the vector defining the position of the point with respect to an arbitrary reference frame and $\vec{E}(\vec{p})$ is the total electric field at point $\vec{p}$. We have thus for the element T_{lk}:

$$Q_{lk} = \rho_{pol}(\vec{p}_k)V_{lk} \tag{9}$$

where $(\vec{p}_k)$ is the representative point of the T_{lk} portion of volume. In the following section this computational scheme will be applied by using for $\epsilon(\vec{p})$ the values obtained by utilizing the local densities $d(r)$ of the solvent drawn for simulations[11,12] with corrections in the case of nonspherical solutes as given by Floris et al.[38] The values of $\epsilon(P,T)$ given in the tables of Archer and Wang[32] are combined then with the relationship density−pressure at a given temperature given by Haar et al.[39] (Those tables are now available in interactive form on the Internet at http://www.geology.washington.edu/ghiorso/MeltsCALC/water.html).

We may thus define an initial guess for the set of AVC, $\{Q^{00}_{T,lk}\}$ using the field $\vec{E}^0(\vec{p})$ produced by the unperturbed solute. We shall then proceed to perform an iterative PCM calculation according to the prescriptions given by Miertuš et al.[19] Density effects on the $G_{dis-rep}$ contributions are also included by modifying the formulas given by Floris et al.[33] (some misprints in the their paper have been corrected by Tomasi and Persico[13]).

4. Results

The reaction has been studied along the symmetric coordinate

$$r_c = R_{CCl} - R_{CCl'}$$

with a fixed *Cl′CCl* 180° angle, in vacuo and with the standard PCM version for the aqueous phase.

The partition of $G(R)$ into components according to eq 1 is reported in Table 3 and Figure 2 (for the SCW1 solvent only). The values reported here are differences with respect to isolated reagents:

$$\Delta G_x(r_c) = G_x(r_c) - G_x(\infty) \tag{10}$$

where x is for any term of eq 1.

The cavity has been defined in terms of Bondi's[40] van der Waals radii multiplied by a factor $f = 1.2$. Additional spheres are computed with the standard parameters of GEPOL.[29] Calculations have been performed with a new set of PCM routines appended to Gaussian94[41] (see Cossi et al.[43] for some comparisons between our PCM and the version of it included in the original release of Gaussian94). All the calculations have been performed with a 6-31G* basis set.

The results reported in Table 2 and Figure 1 show that the reaction profiles in supercritical phases are intermediate between those of AW and in vacuo.

Further consideration are suggested from Table 3 and Figure 2. (1) Cavitation and repulsion dispersion terms have a short-range effect. These terms have no influence on the reaction profile shape. (2) Molecular motion terms have a complex behavior related to the variation of molecular vibrations versus the geometry and symmetry of the molecule. This term has a small influence on the shallow and broad minimum shown by the total curve in Figure 2. (3) The electrostatic term plays a major role: the shape of its curve is very similar to the shape of the total one. It is interesting to partition the electrostatic term

$$G_{el} = \left\langle \Phi \middle| H^0 + \frac{1}{2}V_{el} \middle| \Phi \right\rangle \tag{11}$$

into two parts:

$$EL1 = \frac{1}{2}\langle\Phi|V_{el}|\Phi\rangle \tag{12}$$

and

$$EL2 = \langle\Phi|H^0|\Phi\rangle \tag{13}$$

where V_{el} is the electrostatic potential generated by ASC charges and H^0 is the Hamiltonian of the solute in vacuo. The results of the partition are reported in Table 4 and Figure 3 and compared with the corresponding value in vacuo:

$$E^0 = \langle\Phi^0|H^0|\Phi^0\rangle \tag{14}$$

From this analysis we make the following remarks. (1) Almost all the energy differences between vacuo and SCW1 electrostatics are contained in the EL1 term. It shows a strong and broad maximum at $r_c = 0$. We recall that EL1 is just the reversible work spent to polarize the dielectric under the effect of the solute charge distribution. (2) the EL2 and E^0 values are very close. In Figure 3 E^0 has not been drawn because it is not distinguishable from the EL2 curve. These curves present a maximum at $r_c = 0$ and two minima at $|r_c| = 1.441$. (3) The sum of EL1 and EL2 shows a maximum at $r_c = 0$ with a width of the bell-shaped curve intermediate between those of EL1 and EL2. The minimum at $|r_c| = 1.441$ of E^0 disappears and is replaced by two very shallow minima at $|r_c| \simeq 2$ and $|r_c| \simeq 5$. We recall that the minimum of E^0 corresponds to the molecular

TABLE 2: Free Energy of the System at Several Values of r_c[a]

$\|r_c\|$	in vacuo	AW	SCW1	SCW2	SCW3
5.708	−2.61	−0.18	−1.29	−2.03	−0.43
4.205	−3.66	−0.47	−0.73	−1.97	−0.33
2.697	−6.19	3.39	2.07	−0.33	1.18
1.441	−8.86	6.27	4.97	0.85	2.31
1.124	−7.29	8.86	6.91	2.51	3.53
0.772	−1.89	15.54	13.58	8.67	9.48
0.538	2.04	20.88	18.01	12.65	13.03
0.000	5.60	26.43	25.16	19.32	20.71

[a] Energies in kcal/mol, r_c in Å. Values are given as the difference with respect to $|r_c| = \infty$.

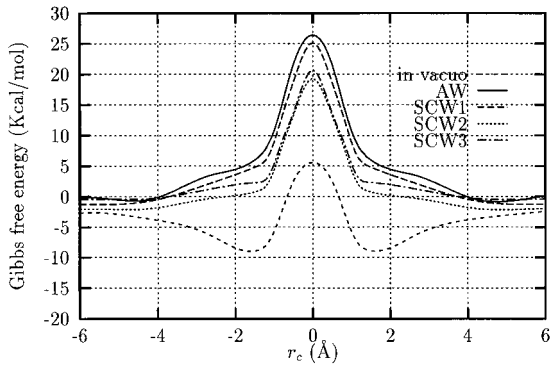

Figure 1. Reaction profiles in various media.

TABLE 3: Components of the Free Energy in SCW1 Solvent with Reference to Reagents[a]

$\|r_c\|$	$\Delta G_{el}(r_c)$	$\Delta G_{cav}(r_c)$	$\Delta G_{dis}(r_c)$	$\Delta G_{rep}(r_c)$	$\Delta G_{Mm}(r_c)$	$\Delta G(r_c)$
5.708	−0.35	0.02	0.06	−0.01	−1.02	−1.29
4.205	−0.44	0.02	0.32	−0.06	−0.59	−0.73
2.697	1.44	0.04	0.76	−0.20	0.03	2.07
1.441	2.56	−0.44	1.01	−0.31	1.99	4.91
1.124	4.87	−1.38	1.05	−0.34	2.70	6.91
0.772	11.08	−2.26	1.09	−0.36	4.02	13.58
0.538	16.90	−2.45	1.11	−0.37	2.81	18.01
0.000	21.93	−1.66	1.10	−0.35	4.13	25.16

[a] Energies in kcal/mol, $|r_c|$ in Å.

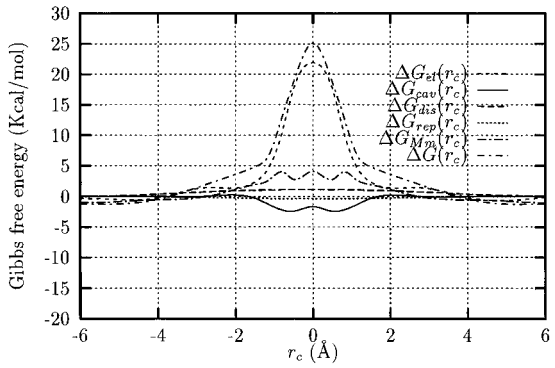

Figure 2. Partition of $\Delta G(r_c)$ for SCW1 in components according to eq 1.

complex Cl:CH_3Cl. The behavior we have found may be tentatively explained as follows. Starting from $|r_c| = \infty$, the electrostatic component of the potential of mean force is negative, as is the energy in vacuo, but screened by the solvent. Near $|r_c| \simeq 3$ the two cavities merge into one, leading to a somewhat less favorable solvation. The solvent-excluded volume described in terms of additional spheres smoothly decreases and reaches zero at $|r_c| \simeq 2.5$. This is a tentative explanation, and we remark that the shape of the curve between $|r_c| = 2$ and 4 is modified by the other terms of the free energy (see Figure 2).

TABLE 4: Partition of the Electrostatic Component of Free Energy in SCW1 and Comparison with That in Vacuo[a]

$\|r_c\|$	EL1 + EL2	EL1	EL2	E^0
5.708	−0.35	2.02	−2.37	−2.37
4.205	−0.44	3.16	−3.60	−3.60
2.697	1.44	7.85	−6.41	−6.41
1.441	2.56	12.82	−10.26	−10.26
1.124	4.87	14.10	−9.23	−9.24
0.772	11.08	15.53	−4.45	−4.45
0.538	16.90	16.84	0.06	0.06
0.000	21.93	18.30	3.63	3.63

[a] r_c in Å. Electrostatic components in kcal/mol.

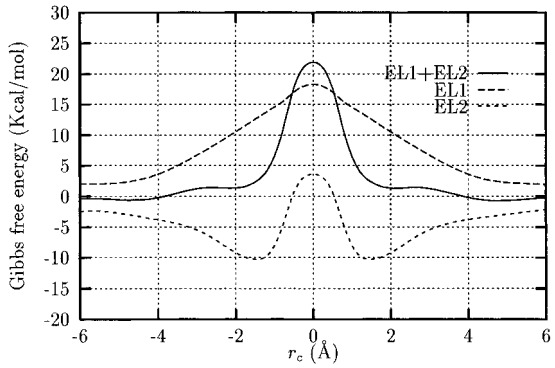

Figure 3. Partition of $\Delta G_{el}(r_c)$ for SCW1 in EL1 and EL2.

TABLE 5: Mulliken Charges in SCW1 Solvent[a]

$\|rc\|$	Cl′	Cl	C	H
∞	−1.000	−0.154	−0.536	0.230
5.708	−1.000	−0.164	−0.532	0.232
4.205	−0.999	−0.169	−0.530	0.233
2.697	−0.998	−0.178	0.521	0.233
1.441	−0.985	−0.221	−0.493	0.233
1.124	−0.976	−0.249	−0.478	0.235
0.772	−0.956	−0.321	−0.456	0.245
0.538	−0.925	−0.422	−0.423	0.257
0.000	−0.775	−0.775	−0.302	0.284

[a] Charges in atomic units, r_c in Å.

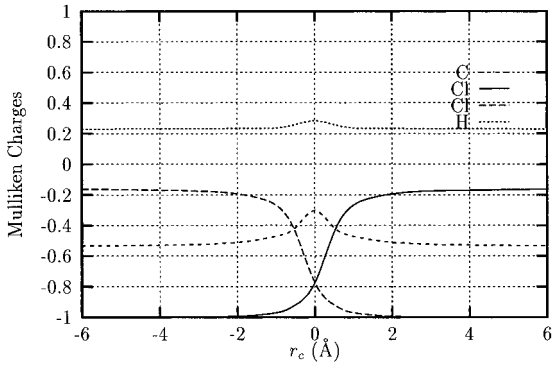

Figure 4. Mulliken charges along the reaction coordinate in SCW1 medium.

The charge transfer in the reaction is shown in Table 5 and Figure 4 where the Mulliken charges in the SCW1 reaction also have been reported. Table 6 reports charge distributions at the transition state for all media. A similar behavior is shown by SCW2, SCW3, and AW reactions.

We shall now examine the effects of geometry optimization in the various media. The regular shape of the energy reaction profile suggests that geometry optimization be limited to reactants and the TS state. In Table 7 we have reported the geometrical parameters for the TS found at the SCF and MP2 levels with all media. The effects on the geometries due to the

TABLE 6: Mulliken Charges at Transition State[a]

solvent	Cl and Cl′	C	H
in vacuo	−0.741	−0.301	0.261
AW	−0.783	−0.295	0.287
SCW1	−0.775	−0.302	0.284
SCW2	−0.760	−0.303	0.274
SCW3	−0.755	−0.307	0.272

[a] Charges in atomic units.

TABLE 7: Optimized Geometries for the Transition State at SCF and MP2 Levels

	SCF		MP2	
solvent	R_{CCl}	R_{CH}	R_{CCl}	R_{CH}
in vacuo	2.383	1.061	2.307	1.072
AW	2.400	1.061	2.303	1.072
SCW1	2.383	1.061	2.290	1.072
SCW2	2.372	1.061	2.285	1.072
SCW3	2.361	1.061	2.281	1.072

TABLE 8: Reaction Barriers in kcal/mol Evaluated at Various Levels of Quantum Theory[a]

solvent	SCF	MP2	MP4	QCISD
in vacuo	5.60	5.61	5.63	7.40
AW	26.23	27.86	27.71	27.15
SCW1	25.10	26.73	26.73	26.20
SCW2	19.53	20.39	20.44	19.90
SCW3	20.70	20.19	20.29	19.76

[a] The geometries refer to SCF and MP2 optimizations in the various media (MP2 geometries also used for MP4 and QCISD).

level of the QM calculation are sizeable, while the effects due to the medium are smaller at both levels of the QM description. It is worth remarking that in SCW R_{CCl} distances are a bit shorter than in AW. Geometries obtained in vacuo with the larger basis set 6.31++G(d,p) are $R_{CCl} = 2.394$, $R_{CH} = 1.062$ at the HF level and $R_{CCl} = 2.316$ and $R_{CH} = 1.072$ in vacuo.[42] For the results of other geometry optimizations in vacuo see Deng et al.[44] and references therein.

The only geometry optimization in ambient water we know of is due to Truong and Stefanovic where use is made of the GCOSMO solvation procedure and of a 6.31+G(d,p) basis set: at the TS, optimized values are $R_{CCl} = 2.396$ and $R_{CH} = 1.062$ at the HF level and $R_{CCl} = 2.311$ and $R_{CH} = 1.069$ at the MP2 level. We recall that GCOSMO is another *ab initio* solvation method similar to the standard version of PCM. By comparison of data in vacuo and in AW with the corresponding results of Table 7, it is shown that the inclusion of a diffuse function does not have a great effect on geometry.

The reaction barrier with SCF and MP2 optimized geometries are reported in Table 8. The MP2 geometry has also been used for MP4[46−48] and QCISD[50] calculations. It appears that, with the 6.31G* basis, the level of the QM description has no large impact.

The numerous calculations in vacuo show a great variance of the barrier in the height with respect to changes of basis set and of QM level (see ref 44 and references therein and in particular the extensive and accurate study of Wladkowsky et al.[49] on a cognate S_N2 reaction).

In all the last-mentioned cases the molecular motion term has also been evaluated at the MP2 level that allows an analytical calculation of frequencies.[51]

The barrier heights we have found are compared in Table 9 with the results obtained with molecular dynamics simulations[11,12] and with the continuum DelPhi method.[16] To make this comparison easier, we convert our results into the form displayed in these papers.

TABLE 9: Comparison with Literature Results

solvent	$\Delta G(0)^a$	$\Delta U_{gas}(0)^a$	$\Delta A(0)^a$	$\Delta A(0)^b$	$\Delta A(0)^c$	$\Delta A(0)^d$	$\Delta A(0)^e$
AW	26.2	7.8	18.4	18.9	16.9	20.9	18.6
SCW1	25.1	5.7	19.4	19.6	17.2	21.0	
SCW2	19.5	5.1	14.4	19.8	12.2	15.2	
SCW3	20.7	5.1	15.6	15.8	10.9	13.6	

[a] Present paper. [b] MD simulation.[12] [c] DelPhi with R and [d] R' radii sets.[16] [e] MC simulation.[27]

The free energy was decomposed in the following way:

$$\Delta G(r_c) = \Delta A(r_c) + \Delta U_{gas}(r_c) \quad (15)$$

ΔA is the charge in free energy in the solution at r_c; ΔA is set equal to zero at a very large value of of $|r_c|$. ΔU_{gas} is the corresponding change in the gas phase; ΔU_{gas} is set equal to zero at a very large value of $|r_c|$. In the quoted papers the attention is focused on ΔA. ΔU_{gas} is considered independent and taken from the 6.31G* SCF calculations of Chandasekar et al.[27] We have decomposed our $\Delta G(r_c)$ values in a similar way, also giving $\Delta U_{gas}(r_c)$ values values defined as

$$\Delta U_{gas}(r_c) = (E^0(r_c) - E^0(\infty)) + (G^{gas}_{Mm}(r_c) - G^{gas}_{Mm}(0)) \quad (16)$$

From the inspection of Table 9, it turns out that our ΔA values lie between the two sets of DelPhi values (the R set of radii corresponds to standard MM, the R' set values optimized in AW solution). Our results agree quite well with the simulation results for AW, SCW1, and SCW3, while there is a remarkable difference for SCW2.

We may conclude that PCM, as well as DelPhi, fails in describing simulation values for this region of the $P-T$ space of SCW. Therefore, we have to pass to the second PCM model.

To apply the PCM version including cybotactic effects, we have drawn the pertinent data from molecular dynamics simulations[11,12] and limited the calculations to reactants and to TS for SCW2. Some simulation data that have not been reported in these papers have been obtained by using the same molecular recipes given in ref 16. The two sets of results are in fair agreement. We report in Figure 5, as an example, the functions $\epsilon(r)$ and $\partial\epsilon(r)/\partial r$ for Cl^- we have derived.

The FEM−PCM procedure has been applied by using the GEPOL definition of tesserae[31] as the starting point for the definition of the V_{lk} volumes. No use has been made of the rigid cavity description in the standard PCM. The region filled by the solute to which a value $\epsilon = 1$ has been assigned is described in terms of the $\epsilon(r)$ profiles. Therefore, there are no ASCs here, only AVCs. The final values of the apparent Q_{lk} are reached within few (i.e., 3−4) iterative cycles. The calculations we shall report here refer to the following values of parameters fixing the partition of the space: $k_{max} = 120$ and $r_{k_{max}} = 5r_0$ with $r_0 = 3$ Å. $r_{k_{max}}$ is a value lying in a region with ϵ equal to the bulk value. Additional increments in k_{max} do not lead to significant variations in the results.

The calculations give no significant cybotactic effects for the neutral reactant CH_3Cl and relatively large contributions for Cl^- and $[Cl-CH_3-Cl]^-$. The most relevant result is an increasing of the barrier height for SCW2 to 25.6 kcal/mol corresponding to $\Delta A = 20.5$ compared with the simulation value $\Delta A = 19.8$. The large difference found between simulation results and standard PCM is therefore almost completely recovered.

5. Discussions and Conclusions

We have here reported some calculations on S_N2 reactions in ambient and supercritical water, making use of the PCM method.

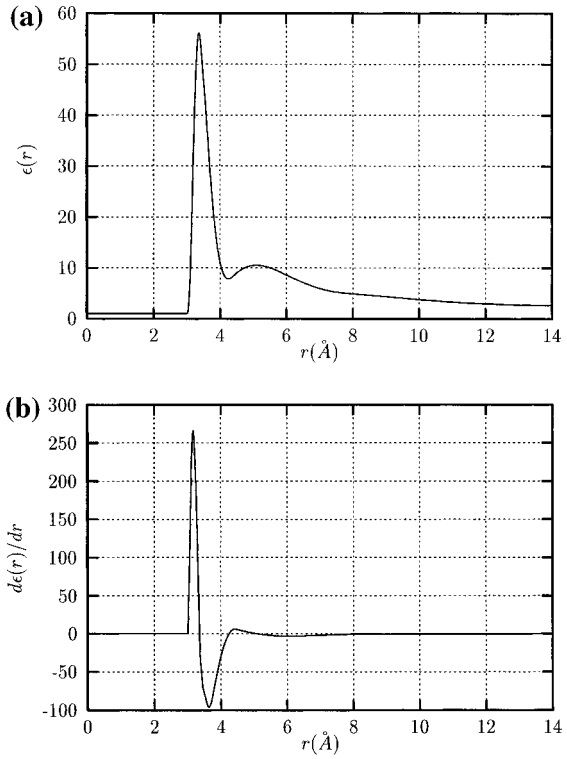

Figure 5. (a) $\epsilon(r)$ and (b) $\partial\epsilon(r)/\partial r$ for Cl^- in SCW2 derived from simulation data.

The main objective of the study was to check if the standard version of PCM, which uses an isotropic and uniform continuum model for the solvent, is also able to describe solvation effects in supercritical water. We have selected this S_N2 reaction because there are some molecular dynamics studies on this reaction in SCW to compare.[11,12] The simulation studies are accompanied by calculations[16] using a classical solvation method indicating that continuum uniform models give a reasonable appreciation of the reaction energy profile and of the barrier height, with the exception of the low-temperature, low-density SCW solvent ($T_r = 1.5$, $d_r = 0.5$).

These findings are confirmed here, where use is made of a QM solvation model. For AW and for SCW1 and SCW3 we found barrier heights within the error of simulation (and of the recommended experimental values for AW) and an error of 5.4 kcal/mol for the SCW2 case. This error is sharply reduced to 0.7 kcal/mol when a modified continuum procedure, able to describe cybotactic effects specific for supercritical fluids, is used.

This procedure, described here for the first time, deserves some discussion. The mathematical formulation is derived from a previous version conceived for ambient solutes. At ambient $P-T$ conditions cybotactic effects due to the two main physical sources of local disturbance of solvent distributions, i.e., electrostriction and dielectric saturation, compensate each other to a good extent. What is left can be easily described by using appropriate cavity radii. This is currently done in the PCM and other continuum uniform solvent models. For cations, especially of molecular type where the extra charge is mainly located in a specific portion of the molecule, it is convenient to introduce a position-dependent dielectric function $\epsilon(\vec{r})$, instead of bringing additional modifications to the cavity radii.

This function $\epsilon(\vec{r})$ actually corresponds to a function depending on the local value of electric field $E(\vec{r})$ because dielectric saturation effects, depending on $\vec{E}$, are predominant terms. The $\epsilon(\vec{r})$ function has a sigmoidal shape, easily modeled in terms of $\vec{E}(\vec{r})$ values using experimental data and results of computer simulations to fix details of functional form and parameters.

In supercritical liquids the experience is more limited. This study and the one reported by Bennet et al.[16] indicate that uniform continuum models with an appropriate choice of radii may describe the energetics of solvation for large portions of the supercritical $P-T$ space. However, there is a region in the SCW phase diagram where this simple recipe fails. This region is characterized by a large isothermal compressibility accompanied by large density fluctuations, which correlate over a long range.

The result is a cybotactic effect dominated by electrostriction, or solvent clustering but with long tails. The definition of a $\epsilon(\vec{r})$ function able to describe this effect is less immediate than in the case of dielectric saturation.

This is why we have used here a strategy that is apparently of little practical use. We have derived our $\epsilon(\vec{r})$ from simulation studies in the attempt to reproduce simulation results. Continuum studies are less expensive than simulation calculations by several orders of magnitude, but to routinely apply the method used here apparently means to perform a simulation study first and then to add continuum calculations. Actually, our study must be considered as a first step to define the appropriate shape for the $\epsilon(\vec{r})$ function. There is a nice continuum model, called the compressible continuum (CC) method, that was elaborated by Luo and Tucker. In the CC method the $\epsilon(\vec{r})$ function is obtained from experimental bulk data with the aid of some numerical calculations based on a model proposed by Frank in 1955 and relates local values of solvent density to the electric field.[52] It is quite likely that, when this CC method is applied to the S_N2 reaction considered here, there will be some reasonable results for the SCW2 case. This hypothetical result would be a good argument for supporting the view that $\epsilon(\vec{r})$ can be modeled by using $d(\vec{r})$ values expressed in terms of the local field $\vec{E}(\vec{r})$ and of isothermal compressibility as in Frank's formula, disregarding other effects. However one has to take into account that numerical compensation of errors often occur and that repeated checks on other systems and the use of independent methods are necessary.

Both CC and DelPhi methods are of classical type. The solvent electric field has as its source a set of fixed charges, generally those derived from Mulliken's population analysis of a QM calculation of a solute in vacuo. This procedure can easily lead to acceptable solvation energies for molecules in their ground state equilibrium geometry (the uncertainly in ΔA for the DelPhi version used by Bennet et al.[16] is about 1 kcal/mol [53]), but extension to the study of reaction mechanism presents some problems. Both experience and theory indicate that QM descriptions of a high level are often necessary; even when the study can be limited to a single diabatic surface, there are often admixtures of other electronic states making the single-determinant description untenable. Both in a single- and in a multideterminant description the effects due to the coupling of solvent polarization to the intrinsic bond-breaking/-forming processes may play a crucial role not adequately described in terms of classical charges derived from in vacuo calculations.[14]

The PCM procedure has several features making it a good candidate for these studies. The uncertainty in ΔG calculation is now reduced to $\sim$0.4 kcal/mol for ground state solutes at equilibrium geometry, using a 6.31G* basis set.[54] The equilibrium geometry in solution can be routinely determined. The method accepts QM description at any level with accurate descriptions of polarization effects due to the medium. It supplements G_{el} with other contributions not described by many other solvation methods.

The S_N2 reaction is an unfortunate choice to show the potential of PCM in describing reaction mechanisms, the molecular system being too simple. The low-level formulation of the QM description we have used here to make comparisons with other calculations more immediate further reduces the demonstration of the advantage of using this method. In fact we have used the single-determinant 6.31G* description of the reaction coordinate used by all other papers we have examined. We have remarked that the quality of the description strongly depends on the QM method and, as many studies on model S_N2 reactions indicate, that the use of diabatic surfaces is almost necessary to have a proper description of the reaction process (see, for example, Hynes et al.[55]). In addition, the molecular system $Cl^- + CH_3Cl$ is too small and rigid to stress the importance of others factors. We have indicated that G_{dis}, G_{rep}, and G_{Mm} terms play a secondary role; it is not said that the same holds for reactions of more complex systems.

The problems for reactions in supercritical liquids are the same, with the additional problem of properly describing local clustering and density fluctuations with long-range correlation. The CC method could turn out to be the good model to describe electrostatic effects, but if this is the case, an implementation at the *ab initio* QM level, similar to PCM, is necessary to study reactions in supercritical water.

Acknowledgment. Financial support of CNR is here acknowledged.

Appendix. ASC Renormalization

Apparent surface charges are obtained in PCM via a coupled solution of the QM and the electrostatic problem. The final result is a set (or two sets, according to the PCM version) of point charges q_i each assigned to a surface tessera of known area a_i.

The surface integral of ASC is thus reduced to a summation

$$Q_{comp} = \sum_{i=1}^{N} q_i \tag{17}$$

According to the Gauss theorem, the ASC integral should be a simple function of the solute charge Q_{int} (of the pertinent portion of it, according to the PCM version):

$$Q_{theor} = -\frac{\epsilon - 1}{\epsilon} Q_{int} \tag{18}$$

Actually, there are differences between Q_{comp} and Q_{theor} due to the combination of two factors, the finite size of BEM tesserae, and the occurrence of solute electronic tails.[31]

We are using a PCM version in which apparent charges due to solute nuclei and electrons are separately treated. We have now two sets of apparent charges, $\{q_i^N\}$ and $\{q_i^e\}$. The first one has an error due to the BEM procedure only. Both sets of charges are renormalized with a simple formula:

$$\tilde{q}^x = q_i^x \frac{Q^x_{theor}}{Q^x_{comp}} \tag{19}$$

When the system is separated into two fragments, the new modification of the program performs separate renormalization of $\{q_i^N\}$ and $\{q_i^e\}$ charges for both fragments. The program is provided with a logical subroutine examining each geometry if there is a separation. If this is the case, the Q^x_{int} values for both fragments are automatically computed in the hypothesis that both fragments are in their ground state and that there is no electron transfer between them (we remember that disconnected systems have at least one solvent molecule between the two).

References and Notes

(1) Klein, M. T.; Torry, L. A. *Ind. Eng. Chem. Res.* **1992**, *31*, 182.
(2) Johnston, K. P. *Nature* **1994**, *368*, 187.
(3) de Pablo, J. J.; Prausnitz, J. M.; Stauch, H. J.; Cummings, P. T. *J. Chem. Phys.* **1990**, *93*, 7355.
(4) Cummings, P. T.; Cochran, H. D.; Simonson, J. M.; Mesmer, R. E.; Karaborni, S. *J. Chem. Phys.* **1991**, *94*, 5607.
(5) Cochran, H. D.; Cummings, P. T.; Karaborni, S. *Fluid Phase Equil.* **1992**, *71*, 1.
(6) Gao, J. *J. Am. Chem. Soc.* **1993**, *115*, 6863.
(7) Guillot, B.; Guissani, Y. *J. Chem. Phys.* **1993**, *99*, 8075.
(8) Balbuena, P. B.; Johnston, K. P.; Rossky, P. J. *J. Am. Chem. Soc.* **1994**, *116*, 2689.
(9) Cui, S. T.; Harris, J. G. *Chem. Eng. Sci.* **1994**, *49*, 2749.
(10) Gao, J. *J. Phys. Chem.* **1994**, *98*, 6049.
(11) Balbuena, P. B.; Johnston, K. P.; Rossky, P. J. *J. Phys. Chem.* **1995**, *99*, 1554.
(12) Flanagin, L. W.; Balbuena, P. B.; Johnston, K. P.; Rossky, P. J. *J. Phys. Chem.* **1995**, *99*, 5196.
(13) Tomasi, J.; Persico, M. *Chem. Rev.* **1994**, *94*, 2027.
(14) Tomasi, J.; Cammi, R.; Cossi, M.; Mennucci, B. In *Theoretical Aspects of Biochemical Reactions*; Náray-Szabó, G., Warshel, A., Eds.; Kluwer: Dordrecht, 1997.
(15) Luo, H.; Tucker, S. C. *J. Phys. Chem.* **1996**, *100*, 11165.
(16) Bennet, G. E.; Rossky, P. J.; Johnston, K. P. *J. Phys. Chem.* **1995**, *99*, 16136.
(17) Tucker, S. C.; Gibbons, E. M. In *Structure and Reactivity of Acqueous Solution*; Cramer, C. J., Truhlar, D. G., Eds.; ACS Symposium Series 568; American Chemical Society: Washington, DC, 1994.
(18) Honig, B.; Sharp, K.; Yang, A. S. *J. Phys. Chem.* **1993**, *97*, 1101.
(19) Miertuš, S.; Scrocco, E.; Tomasi, J. *Chem. Phys.* **1981**, *55*, 117.
(20) Cossi, M.; Mennucci, B.; Tomasi, J. *Chem. Phys. Lett.* **1994**, *228*, 165.
(21) Alemán, C.; Maseras, F.; Lledós, A.; Duran, M.; Bertrán, J. *J. Phys. Org. Chem.* **1989**, *2*, 611.
(22) Tomasi, J. *Int. J. Quantum Chem. Symp.* **1991**, *18*, 73.
(23) Bianco, R.; Miertûs, S.; Persico, M.; Tomasi, J. *Chem. Phys.* **1992**, *168*, 281.
(24) Aguilar, M.; Bianco, R.; Miertûs, S.; Persico, M.; Tomasi, J. *Chem. Phys.* **1993**, *174*, 397.
(25) Bianco, R. Doctoral Thesis, Pisa, Italy, 1993.
(26) Basilevsky, M.; Chudinov, G. E.; Napolov, D. V. *J. Phys. Chem.* **1993**, *97*, 3270.
(27) Chandrasekhar, J.; Smith, S. F.; Jorgensen, W. L. *J. Am. Chem. Soc.* **1985**, *107*, 154.
(28) Tomasi, J. In *Structure Reactivity in Acqueous Solution*; Cramer, C. J., Thrular, D. G., Eds.; ACS Symposium Series 568; American Chemical Society: Washington, DC, 1994.
(29) Pascual-Ahuir, J. L.; Silla, E.; Tomasi, J.; Bonaccorsi, R. *J. Comput. Chem.* **1987**, *8*, 778.
(30) Pascual-Ahuir, J. L.; Silla, E.; Tuñon, I. *J. Comput. Chem.* **1994**, *15*, 1127.
(31) Cammi, R.; Tomasi, J. *J. Comput. Chem.* **1995**, *16*, 1449.
(32) Archer, D. G.; Wang, P. *J. Phys. Chem. Ref. Data* **1990**, *19*, 371.
(33) Floris, F. M.; Tomasi, J.; Pascual-Auhir, J. L. *J. Comput. Chem.* **1991**, *12*, 784.
(34) Langlet, J.; Claverie, P.; Caillet, J.; Pullman, A. *J. Phys. Chem.* **1988**, *92*, 1617.
(35) Boskos, D. E. *Boundary elements in mechanics*; North Holland: Amsterdam, 1987; Chapter 2.
(36) Cossi, M.; Mennucci, B.; Tomasi, J. *Chem. Phys. Lett.* **1994**, *228*, 165.
(37) Cossi, M.; Mennucci, B.; Tomasi, J. *J. Chem. Phys.* **1995**, *102*, 6837.
(38) Floris, F. M.; Tani, A.; Tomasi, J. *Chem. Phys.* **1993**, *169*, 11.
(39) Haar, L.; Gallagher, J. S.; Kell, G. S. *NBS/NRC Steam Tables. Thermodynamic and Transport Properties and Computer Programs for Vapor and Liquid States of Water in SI Units*; Hemisphere Publishing Co.: Washington, DC, 1984; pp 271−276.
(40) Bondi, A. *J. Phys. Chem.* **1964**, *68*, 441.
(41) Frisch, M. J.; Trucks, G. W.; Schlegel, H. B.; Gill, P. M. W.; Johnson, B. G.; Robb, M. A.; Cheeseman, J. R.; Keith, T.; Petersson, G. A.; Montgomery, J. A.; Raghavachari, K.; Al-Laham, M. A.; Zakrzewski, V. G.; Ortiz, J. V.; Foresman, J. B.; Peng, C. Y.; Ayala, P. Y.; Chen, W.; Wong, M. W.; Andres, J. L.; Replogle, E. S.; Gomperts, R.; Martin, R. L.; Fox, D. J.; Binkley, J. S.; Defrees, D. J.; Baker, J.; Stewart, J. P.; Head-Gordon, M.; Gonzalez, C.; Pople, J. A. *Gaussian 94*, Revision B.3; Gaussian, Inc.: Pittsburgh, PA, 1995.
(42) Shi, Z.; Boyd, R. J. *J. Am. Chem. Soc.* **1990**, *112*, 6789.

(43) Cossi, M.; Barone, V.; Cammi, R.; Tomasi, J. *Chem. Phys. Lett.* **1990**, *255*, 327.
(44) Deng, L.; Branchadell, V.; Ziegler, T. *J. Am. Chem. Soc*. **1994**, *116*, 10645.
(45) Truong, T. N.; Stefanovic, E. V. *J. Phys. Chem*. **1995**, *99*, 14700.
(46) Møller, C.; Plesset, M. S. *Phys. Rev.* **1934**, *46*, 618.
(47) Saebo, S.; Almlof, J. *Chem. Phys. Lett.* **1989**, *154*, 83.
(48) Krishnan, R.; Pople, J. A. *Int. J. Quantum Chem*. **1978**, *14*, 91.
(49) Wladkowski, B. D.; Lim, K. F.; Allen, W. D.; Brammon, J. I. *J. Am. Chem. Soc*. **1992**, *114*, 9136.
(50) Pople, J. A.; Head-Gordon, M.; Raghavachari, K. *J. Chem. Phys*. **1987**, *87*, 5968.
(51) Head-Gordon, M.; Head-Gordon, T. *Chem. Phys. Lett*. **1994**, *220*, 122.
(52) Frank, H. S. *J. Chem. Phys*. **1955**, *23*, 2023.
(53) Simonson, T.; Brümger, A. *J. Phys. Chem*. **1994**, *98*, 4683.
(54) Barone, V.; Cossi, M.; Tomasi J. To be published.
(55) Mathis, J. R.; Bianco, R.; Hynes, J. T. *J. Mol. Liq*. **1995**, *99*, 17516.